Y. Shi
State Key Laboratory of Mechanics and Control of Mechanical Structures, Nanjing University of Aeronautics and Astronautics, Nanjing 210016, China; Department of Civil and Environmental Engineering, Department of Mechanical Engineering, Center for Engineering and Health, Skin Disease Research Center, Northwestern University, Evanston, IL 60208

C. Dagdeviren
Department of Materials Science and Engineering, Frederick Seitz Materials Research Laboratory, University of Illinois at Urbana–Champaign, Urbana, IL 61801

J. A. Rogers
Department of Materials Science and Engineering, Frederick Seitz Materials Research Laboratory, University of Illinois at Urbana–Champaign, Urbana, IL 61801

C. F. Gao
State Key Laboratory of Mechanics and Control of Mechanical Structures, Nanjing University of Aeronautics and Astronautics, Nanjing 210016, China

Y. Huang[1]
Department of Civil and Environmental Engineering, Department of Mechanical Engineering, Center for Engineering and Health, Skin Disease Research Center, Northwestern University, Evanston, IL 60208
e-mail: y-huang@northwestern.edu

An Analytic Model for Skin Modulus Measurement Via Conformal Piezoelectric Systems

The Young's modulus of human skin is of great interests to dermatology, cutaneous pathology, and cosmetic industry. A wearable, ultrathin, and stretchable device provides a noninvasive approach to measure the Young's modulus of human skin at any location, and in a way that is mechanically invisible to the subject. A mechanics model is developed in this paper to establish the relation between the sensor voltage and the skin modulus, which, together with the experiments, provides a robust way to determine the Young's modulus of the human skin. [DOI: 10.1115/1.4030820]

Keywords: skin modulus, piezoelectric actuators and sensors, analytic model

1 Introduction

Human skin plays an essential role in protecting the organism from the environment. Change in its mechanical properties reflects the tissue modifications caused by aging, disease, or stimulation of the environments [1]. The mechanical properties of human skin, such as the Young's modulus, are of great interests to dermatology, cutaneous pathology, and cosmetic industry [2].

The Young's modulus of human skin has been obtained from the linear elastic part of the stress–strain curve [3]. The stress–strain curve is measured by one of the following three techniques: (1) twist of the skin [3], (2) indentation [2], and (3) method of suction [4]. These tests, however, all involve relatively complex setup in the laboratory, which prevent simple and portable applications outside the lab. In addition, such tests involve relatively large deformation of the skin, and therefore are difficult to repeat quickly because it takes hours for the skin distortion to disappear upon unloading [3].

Dagdeviren et al. [5] developed a wearable, ultrathin, and stretchable modulus measurement device that is much more robust than the existing techniques. The device consists of a series of microflexible lead zirconate titanate (PZT) [6] actuators and sensors laminated on a thin elastomeric matrix. It provides a noninvasive approach to measure the Young's modulus of human skin at any location, normal conditions and upon administration of pharmacological and moisturizing agents, and in a way that is mechanically invisible to the subject. As to be shown in the analytic model in Sec. 2, the Young's modulus of human skin is linearly proportional to the sensor's output voltage (for each given actuating voltage). Therefore, the measured output voltage, together with the analytic model, determines the Young's modulus of human skin.

[1]Corresponding author.
Contributed by the Applied Mechanics Division of ASME for publication in the JOURNAL OF APPLIED MECHANICS. Manuscript received April 4, 2015; final manuscript received April 13, 2015; published online June 25, 2015. Editor: Arun Shukla.

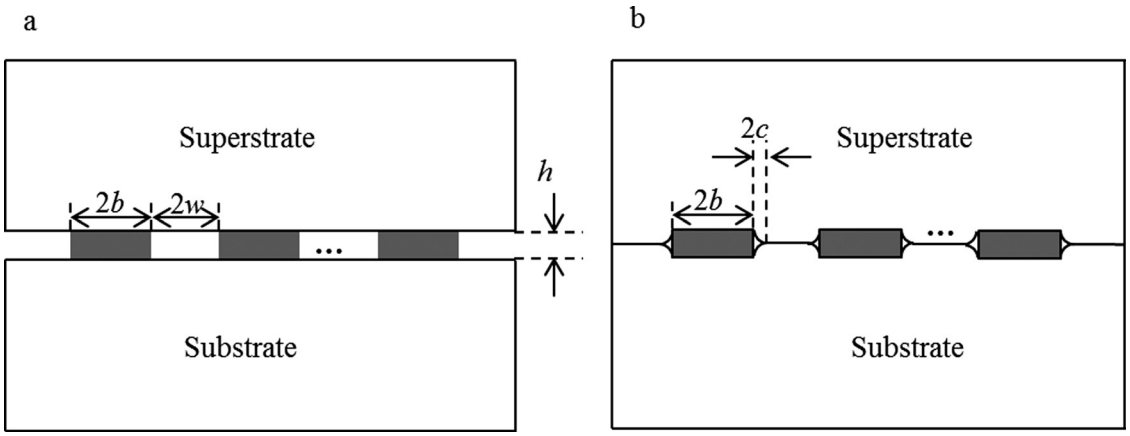

Fig. 1 An array of PZT ribbons sandwiched by the super- and substrates. (*a*) A schematic diagram and (*b*) the super- and substrates adhere together to form air-gaps at each end of the PZT ribbon.

The objective of this paper is to establish an analytic model in Sec. 2, particularly the linear relation between the sensor's output voltage and the Young's modulus. The analytic model is validated in Sec. 3, and the application of this model to human skin is discussed in Sec. 4.

2 An Analytic Model

Figure 1(*a*) shows an array of n PZT ribbons sandwiched by two semi-infinite media (the super- and substrates are much thicker than the PZT ribbons). The thickness h of PZT ribbons is much smaller than their width $2b$ and spacing $2w$ such that the substrate and superstrate adhere over the parts without the PZT ribbon, as illustrated in Fig. 1(*b*). This leaves an air-gap at each terminal of the PZT ribbon, where the length $2c$ of air-gap is to be determined by the work of adhesion between two media [7], as given at the end of this section. Each PZT ribbon, together with the two air-gaps around its ends, can be modeled as an interfacial crack with the length $2b+4c$, with the center part (length $2b$) in contact with the PZT ribbon.

One PZT ribbon is subjected to an actuating voltage U_A. Without the surrounding media, it would expand freely by (see the Appendix)

$$\Delta u = \frac{c_{11}e_{33} - c_{13}e_{31}}{c_{11}c_{33} - c_{13}^2} U_A \tag{1}$$

due to piezoelectricity of PZT, where c_{ij} and e_{ij} are the elastic and piezoelectric constants of PZT, respectively, given in the Appendix. The expansion of this PZT ribbon with the actuating voltage causes deformation in the surrounding media, of which the elastic moduli are several orders of magnitude smaller than that of PZT. As a result, the contraction of this PZT ribbon with the actuating voltage due to deformation in the surrounding media is negligible as compared to Δu, as shown in the Appendix. Therefore, the boundary conditions for this crack, due to actuating voltage U_A, are the constant opening displacement Δu in the center part (of length $2b$) and traction free around the two ends (each of length $2c$), as illustrated in Fig. 2(*a*).

The deformation in the surrounding media, in turn, causes the other PZT ribbons (without the actuating voltage) to expand. Let $U_{S,i}$ denote the sensing voltage in the ith PZT ribbon, which is several orders of magnitude smaller than U_A, as shown in the Appendix, such that the deformation induced by $U_{S,i}$ is also negligible. Therefore, the boundary conditions for these cracks, due to actuating voltage U_A, are the vanishing opening displacement in the center part (of length $2b$) and traction free around the two ends (each of length $2c$), as illustrated in Fig. 2(*a*). In fact, such a crack (of length $2b+4c$) can be considered as two smaller cracks (each of length $2c$) since the center part (of length $2b$) does not open up.

The above problem (illustrated in Fig. 2(*a*)) can be decomposed to the following two subproblems:

(1) A single crack (of length $2b+4c$) subjected to the opening displacement in Eq. (1) over the center part (of length $2b$), which is modeled as a crack with a rigid wedge (Fig. 2(*b*)).
(2) The collinear cracks (each of length $2c$) subjected crack-face pressure to negate the normal tractions on the crack face induced by 1), as illustrated in Fig. 2(*c*), such as the air-gap remain traction free.

For the first subproblem illustrated in Fig. 2(*b*), the Westergaard function is given by [8]

$$Z^{\Delta u}(z) = \frac{E'(b+2c)\Delta u}{4K\left[\sqrt{1-\dfrac{b^2}{(b+2c)^2}}\right]} \frac{1}{\sqrt{z^2-(b+2c)^2}} \frac{1}{\sqrt{z^2-b^2}} \tag{2}$$

where E' is the plane-strain, effective modulus of the media and is to be discussed in detail at the end of this section, $K(k) = \int_0^{\pi/2} \left(1-k^2\sin^2\varphi\right)^{-1/2} d\varphi$ is the complete elliptic integral of first kind, $z = x+iy$, with $i=\sqrt{-1}$ and (x, y) is the local coordinate with the origin at the center of the crack. The normal stress along the crack line ($y=0$) is given by

$$\sigma_y^{\Delta u}(x) = \begin{cases} \dfrac{E'(b+2c)\Delta u}{4K\left[\sqrt{1-\dfrac{b^2}{(b+2c)^2}}\right]\sqrt{\left[x^2-(b+2c)^2\right](x^2-b^2)}}, & |x| > b+2c \\ 0, & b < |x| < b+2c \end{cases} \tag{3}$$

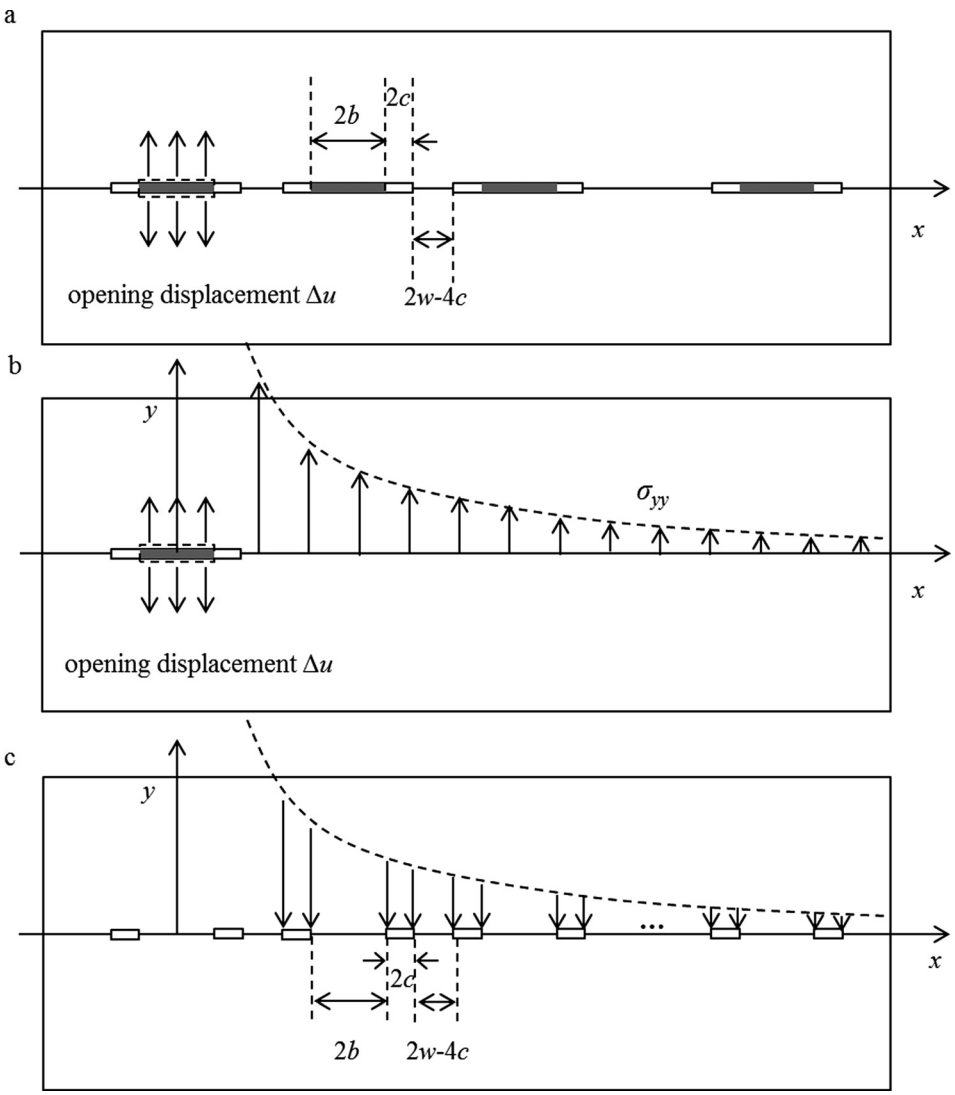

Fig. 2 A schematic illustration of the mechanics model. (*a*) PZT ribbons with air-gaps, with one of them (actuator) subjected to the actuating voltage, which results expansion in the actuator and therefore opening displacement at the interface between the adhered super- and substrates. (*b*) Subproblem 1, a single crack, representing the actuator and its two air-gaps, subjected to the opening displacement. (*c*) Subproblem 2, negation of the normal tractions induced by subproblem 1 at all air-gaps.

where 0 in the second line represents the vanishing normal stress traction over two air-gaps around the PZT subjected to the actuating voltage U_A.

For the second subproblem illustrated in Fig. 2(*c*), the collinear cracks have the length $2c$ and center-to-center spacing alternating between $d_1 = 2b + 2c$ and $d_2 = 2w - 2c$. As shown at the end of this section, the air-gap is much shorter than the spacing d_1 and d_2 such that the normal stress to be negated on the jth crack can be approximated by the corresponding value at the center ($x = x_j$ and $y = 0$) of the crack, i.e.,

$$p_j = \begin{cases} -\dfrac{E'(b+2c)\Delta u}{4K\left[\sqrt{1-\dfrac{b^2}{(b+2c)^2}}\right]\sqrt{\left[x_j^2-(b+2c)^2\right]\left(x_j^2-b^2\right)}}, & |x_j| > b+2c \\ 0, & b < |x_j| < b+2c \end{cases} \tag{4}$$

where $1 \le j \le 2n$ (n is the number of PZT ribbons), the negative sign in the first line of Eq. (4) denotes the negation. The Westergaard function for the second subproblem is then given by [9,10]

$$Z(z) = \frac{1}{\prod_{k=1}^{2n}\left[(z-x_k)^2-c^2\right]^{1/2}} \sum_{j=1}^{2n}\left[\frac{(-1)^{j-1}p_j}{\pi}\int_{x_j-c}^{x_j+c}\frac{\prod_{k=1}^{2n}\left|(\xi-x_k)^2-c^2\right|^{1/2}}{z-\xi}d\xi + a_{j-1}z^{j-1}\right] \tag{5}$$

where $2n$ is the total number of air-gaps around n PZT ribbons, and the coefficients a_j for the polynomial are determined by the single valued condition of displacement for each crack

$$\oint_{\Gamma_j} \mathrm{Im}[Z(x)]dx = 0 \tag{6}$$

Here, Γ_j $(1 \le j \le 2n)$ is the closed loop for the jth crack. The sum of integrals for $1 \le j \le 2n$ is equivalent to $a_{2n-1} = 0$ [9].

The normal stress along the line $y = 0$ is given by [8]

$$\sigma_y(x) = \mathrm{Re}[Z(x)] \tag{7}$$

It gives the average pressure q_i at the ith sensor as

$$q_i = \frac{1}{2b}\int_{x_{2i-1}+c}^{x_{2i}-c} \left[\sigma_y(x) + \sigma_y^{\Delta u}(x)\right]dx \tag{8}$$

The corresponding output voltage $U_{S,i}$ at the ith sensor is then obtained as (see the Appendix for details)

$$U_{S,i} = h\left|\frac{q_i}{e_{33} + \dfrac{c_{33}e_{31} - c_{13}e_{33}}{c_{11}e_{33} - c_{13}e_{31}}e_{31} + \dfrac{c_{11}c_{33} - c_{13}^2}{c_{11}e_{33} - c_{13}e_{31}}k_{33}}\right| \tag{9}$$

where k_{33} is the dielectric constant of PZT given in the Appendix.

For the incompressible super- and substrates that sandwich the PZT ribbons, the plane-strain, effective modulus E' of the media is given by [7]

$$E' = \frac{2}{\dfrac{1}{E'_{\mathrm{super}}} + \dfrac{1}{E'_{\mathrm{sub}}}} \tag{10}$$

where E'_{super} and E'_{sub} are the plane-strain moduli of the super- and substrates, respectively. The length of air-gap is governed by the competition between the deformation energy (due to adherence of the super- and substrates) and adhesion energy and is given analytically by [7]

$$2c = \frac{E'h^2}{8\pi\gamma} \tag{11}$$

where γ is the work of adhesion between the super and substrates. For the super- and substrates moduli around 0.1 MPa, and a representative work of adhesion 50.6 mJ/m^2 [7], the length of air-gap is on the order of 1 μm, which is much smaller than the width of the sensor (200 μm).

3 Special Case: One Actuator and One Sensor

The special case of two PZT ribbons, with the left and right ones serving as the actuator and sensor, respectively, is considered in this section to further illustrate the analysis. There are four collinear cracks (two air-gaps for each PZT ribbon), and their centers have the coordinates (with the origin at the center of the actuator)

$$\begin{aligned} &x_1 = -b - c, \quad x_2 = b + c, \quad x_3 = b + 2w - c, \\ &x_4 = 3b + 2w + c \end{aligned} \tag{12}$$

Equation (4) then becomes

$$p_1 = p_2 = 0, \quad p_3 \approx -\frac{E'b\Delta u}{8\pi w(b+w)}, \quad p_4 = -\frac{E'b\Delta u}{8\pi(b+w)(2b+w)} \tag{13}$$

for small air-gap length $c \ll b, w$, i.e., only the nonzero pressure p_3 and p_4 need to be considered. Accordingly, the Westergaard function in Eq. (5) can be written as the sum of those for p_3 and p_4, $Z(z) = Z_3(z) + Z_4(z)$, where

$$\begin{aligned} Z_3(z) &= \frac{1}{\prod_{k=1}^{4}\left[(z-x_k)^2 - c^2\right]^{1/2}}\left[\frac{p_3}{\pi}\int_{x_3-c}^{x_3+c}\frac{\prod_{k=1}^{4}\left|(\xi-x_k)^2 - c^2\right|^{1/2}}{z-\xi}d\xi + a_0^{(3)} + a_1^{(3)}z + a_2^{(3)}z^2\right] \\ Z_4(z) &= \frac{1}{\prod_{k=1}^{4}\left[(z-x_k)^2 - c^2\right]^{1/2}}\left[-\frac{p_4}{\pi}\int_{x_4-c}^{x_4+c}\frac{\prod_{k=1}^{4}\left|(\xi-x_k)^2 - c^2\right|^{1/2}}{z-\xi}d\xi + a_0^{(4)} + a_1^{(4)}z + a_2^{(4)}z^2\right] \end{aligned} \tag{14}$$

where the vanishing coefficient $a_3 = 0$ for z^3 has been used. For $c \ll b, w$, Eq. (14) can be simplified to

$$\begin{aligned} Z_3(z) &= \frac{1}{\prod_{k=1}^{4}\left[(z-x_k)^2 - c^2\right]^{1/2}}\left[-\frac{E'b^2\Delta u}{\pi^2}\int_{x_3-c}^{x_3+c}\frac{\left|(\xi-x_3)^2 - c^2\right|^{1/2}}{z-\xi}d\xi + a_0^{(3)} + a_1^{(3)}z + a_2^{(3)}z^2\right] \\ Z_4(z) &= \frac{1}{\prod_{k=1}^{4}\left[(z-x_k)^2 - c^2\right]^{1/2}}\left[\frac{E'b^2\Delta u}{\pi^2}\int_{x_4-c}^{x_4+c}\frac{\left|(\xi-x_4)^2 - c^2\right|^{1/2}}{z-\xi}d\xi + a_0^{(4)} + a_1^{(4)}z + a_2^{(4)}z^2\right] \end{aligned} \tag{15}$$

Here, the coefficients $a_j^{(3)}$ $(j = 0,\ 1,\ \text{and}\ 2)$ are determined by the single valued condition in Eq. (5) around the cracks 1, 2, and 4 but not crack 3 (to avoid a singular, Cauchy-principle integral) because the equivalent condition $a_3 = 0$ for z^3 has already been imposed in Eq. (15). This gives

$$a_0^{(3)} + a_1^{(3)} x_1 + a_2^{(3)} x_1^2 = -\frac{E' b^2 \Delta u}{4\pi(b+w)} c^2$$
$$a_0^{(3)} + a_1^{(3)} x_2 + a_2^{(3)} x_2^2 = -\frac{E' b^2 \Delta u}{4\pi w} c^2 \tag{16}$$
$$a_0^{(3)} + a_1^{(3)} x_4 + a_2^{(3)} x_4^2 = \frac{E' b \Delta u}{4\pi} c^2$$

Similarly, the coefficients $a_j^{(4)}$ ($j=0$, 1, and 2) are determined by the single valued condition in Eq. (5) around the cracks 1, 2, and 3. The resulting $a_j^{(3)}$ and $a_j^{(4)}$ are linear proportional to $c^2 \Delta u$.

The average pressure on the sensor is then obtained from Eqs. (7) and (8) as

$$q_2 = \frac{1}{2b} \int_{x_3+c}^{x_4-c} \left\{ \mathrm{Re}[Z_3(x) + Z_4(x)] + \sigma_y^{\Delta u}(x) \right\} dx \tag{17}$$

where

$$Z_3(x) = \frac{\dfrac{E' b^2 \Delta u}{\pi^2} \displaystyle\int_{x_3-c}^{x_3+c} \frac{\left|(\xi - x_3)^2 - c^2\right|^{1/2}}{x - \xi} d\xi - a_0^{(3)} - a_1^{(3)} x - a_2^{(3)} x^2}{(x-x_1)(x-x_2)\left[(x-x_3)^2 - c^2\right]^{1/2}\left[(x_4-x)^2 - c^2\right]^{1/2}}$$
$$Z_4(x) = \frac{-\dfrac{E' b^2 \Delta u}{\pi^2} \displaystyle\int_{x_4-c}^{x_4+c} \frac{\left|(\xi - x_4)^2 - c^2\right|^{1/2}}{x - \xi} d\xi - a_0^{(4)} - a_1^{(4)} x - a_2^{(4)} x^2}{(x-x_1)(x-x_2)\left[(x-x_3)^2 - c^2\right]^{1/2}\left[(x_4-x)^2 - c^2\right]^{1/2}} \tag{18}$$

which are much smaller than $\sigma_y^{\Delta u}(x)$ for $c \ll b, w$ such that Eq. (17) can be approximated by

$$q_2 \approx -\frac{E' \Delta u}{8\pi b} \ln\left[1 - \frac{b^2}{(b+w)^2}\right] \tag{19}$$

The sensor voltage in Eq. (9) then becomes

$$U_S = U_A \frac{E'}{4\pi} \frac{h}{2b} \frac{\dfrac{c_{11}e_{33} - c_{13}e_{31}}{c_{11}c_{33} - c_{13}^2}}{e_{33} + \dfrac{c_{33}e_{31} - c_{13}e_{33}}{c_{11}e_{33} - c_{13}e_{31}} e_{31} + \dfrac{c_{11}c_{33} - c_{13}^2}{c_{11}e_{33} - c_{13}e_{31}} k_{33}} \ln \frac{1}{1 - \dfrac{b^2}{(b+w)^2}} \tag{20}$$

It is linearly proportional to the actuator voltage U_A, the effective modulus E', and the thickness to width ratio $h/(2b)$ of PZT. It also depends on the material properties of PZT, and the spacing to width ratio w/b through $\ln[1 - b^2/(b+w)^2]^{-1}$. Figure 3 shows this function versus $(b+w)/b$, which decreases rapidly as the spacing increases. Here, $(b+w)/b$ is the ratio of center-to-center distance between the actuator to sensor to the sensor width. It is noted that Eq. (20) is independent of the air-gap length $2c$ for $c \ll b, w$.

The ratio of sensor to actuator voltage U_S/U_A, together with the material parameters of PZT and thickness to width ratio $h/(2b)$ and spacing to width ratio w/b, gives the effective modulus E', and therefore the substrate modulus (if the superstrate modulus is known).

4 Approximate Solution for Multiple Actuators and Sensors

The analysis in Sec. 3 clearly suggests that, for $c \ll b, w$, $Z_3(x) + Z_4(x)$ resulting from the second subproblem in Sec. 2 is negligible as compared to $\sigma_y^{\Delta u}(x)$ resulting from the first subproblem. This observation also holds for multiple sensors such that the average pressure on the ith sensor in Eq. (8) becomes

$$q_i \approx \frac{1}{2b} \int_{x_{2i-1}+c}^{x_{2i}-c} \sigma_y^{\Delta u}(x) dx \approx -\frac{E' \Delta u}{8b\pi} \ln\left[1 - \frac{b^2}{m^2(b+w)^2}\right] \tag{21}$$

where m is the number of sensor away from the actuator, and $m=1$ degenerates to Sec. 3. The voltage in Eq. (9) for all sensors then becomes

$$U_S = U_A \frac{E'}{4\pi} \frac{h}{2b} \frac{\dfrac{c_{11}e_{33} - c_{13}e_{31}}{c_{11}c_{33} - c_{13}^2}}{e_{33} + \dfrac{c_{33}e_{31} - c_{13}e_{33}}{c_{11}e_{33} - c_{13}e_{31}} e_{31} + \dfrac{c_{11}c_{33} - c_{13}^2}{c_{11}e_{33} - c_{13}e_{31}} k_{33}} \ln \frac{1}{1 - \dfrac{b^2}{m^2(b+w)^2}} \tag{22}$$

It has the same relation with U_A, E', $h/(2b)$, and the material properties of PZT as Eq. (20), but now depends on m (the number of sensor away from the actuator) through the ratio $m(b+w)/b$, which is the ratio of center-to-center distance between the actuator to sensor to the sensor width. As shown in Fig. 3, $D = \ln\left\{1 - [m(b+w)/b]^{-2}\right\}^{-1}$ [versus $m(b+w)/b$] decreases

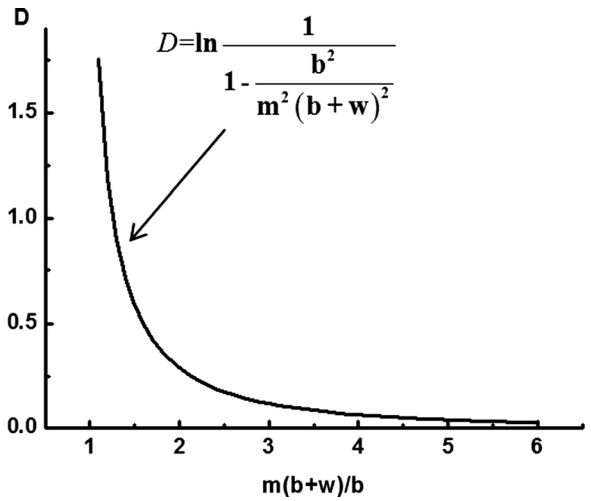

Fig. 3 The function $\ln\{1-[m(b+w)/b]^{-2}\}^{-1}$, which the sensor voltage is linearly proportional to, versus its variable $m(b+w)/b$

rapidly as the number of sensor away from the actuator m increases. Similar to Eq. (20), Eq. (20) is also independent of the air-gap length $2c$ for $c \ll b, w$.

5 Conclusions

Analytic expressions of the sensor voltage are obtained for an array of piezoelectric actuators and sensors between super- and substrates. Together with experimentally measured sensor voltage [5] and the material properties and geometric parameters of piezoelectric actuators and sensors, these expressions provide a simple way to determine the Young's modulus of the substrate if that of the superstrate is known. This is particularly useful to determine the Young's modulus of the skin, as demonstrated in recent experiments [5].

Acknowledgment

Y.S. was partially supported by the National Basic Research Program of China (No. 2015CB351900) and the National Natural Science Foundation (NNSF) of China (No. 11320101001). C.D. and J.A.R. acknowledge the support from the U.S. DOE, Office of Basic Energy Sciences, Division of Materials Sciences and Engineering (No. DE-FG02-07ER46471), through the Frederick Seitz Materials Research Laboratory at the University of Illinois at Urbana-Champaign. C.F.G. acknowledges the support from NNSF (Nos. 11472130 and 11232007). Y.H. acknowledges the support from U.S. National Science Foundation (No. CMMI-1400169).

Appendix

The constitutive model of piezoelectric material gives [11]

$$\begin{Bmatrix}\sigma_{11}\\ \sigma_{22}\\ \sigma_{33}\\ \sigma_{23}\\ \sigma_{31}\\ \sigma_{12}\end{Bmatrix}=\begin{bmatrix}c_{11}&c_{12}&c_{13}&0&0&0\\ c_{12}&c_{11}&c_{13}&0&0&0\\ c_{13}&c_{13}&c_{33}&0&0&0\\ 0&0&0&c_{44}&0&0\\ 0&0&0&0&c_{44}&0\\ 0&0&0&0&0&(c_{11}-c_{12})/2\end{bmatrix}\begin{Bmatrix}\varepsilon_{11}\\ \varepsilon_{22}\\ \varepsilon_{33}\\ 2\varepsilon_{23}\\ 2\varepsilon_{31}\\ 2\varepsilon_{12}\end{Bmatrix}-\begin{bmatrix}0&0&e_{31}\\ 0&0&e_{31}\\ 0&0&e_{33}\\ 0&e_{15}&0\\ e_{15}&0&0\\ 0&0&0\end{bmatrix}\begin{Bmatrix}E_1\\ E_2\\ E_3\end{Bmatrix} \tag{A1}$$

$$\begin{Bmatrix}D_1\\ D_2\\ D_3\end{Bmatrix}=\begin{bmatrix}0&0&0&0&e_{15}&0\\ 0&0&0&e_{15}&0&0\\ e_{31}&e_{31}&e_{33}&0&0&0\end{bmatrix}\begin{Bmatrix}\varepsilon_{11}\\ \varepsilon_{22}\\ \varepsilon_{33}\\ 2\varepsilon_{23}\\ 2\varepsilon_{31}\\ 2\varepsilon_{12}\end{Bmatrix}+\begin{bmatrix}k_{11}&0&0\\ 0&k_{22}&0\\ 0&0&k_{33}\end{bmatrix}\begin{Bmatrix}E_1\\ E_2\\ E_3\end{Bmatrix} \tag{A2}$$

where σ_{ij}, ε_{ij}, E_i, and D_i represent the stress, strain, electrical field, and electrical displacement, respectively, c_{ij}, e_{ij}, and k_{ij} are the elastic, piezoelectric, and dielectric parameters of the material, and the subscript "3" denotes the polarization (vertical, Fig. 2(*a*)) direction of the PZT layer.

The electric field in polarization direction is $E_3^a = U_A/h$ when the PZT ribbon is subjected to the actuating voltage U_A, where the superscript a denotes the actuator. Under plane-strain deformation $\varepsilon_{22}^a = \varepsilon_{12}^a = \varepsilon_{23}^a = 0$, electric field boundary condition $E_1^a = E_2^a = 0$ and the approximate traction free condition $\sigma_{33}^a = 0$ (by neglecting the traction from the soft super- and substrates), Eq. (A1) gives

$$\begin{cases}\sigma_{11}^a = \dfrac{(c_{11}c_{33}-c_{13}^2)\varepsilon_{11}^a + (c_{13}e_{33}-c_{33}e_{31})E_3^a}{c_{33}}\\ \varepsilon_{33}^a = \dfrac{e_{33}E_3^a - c_{13}\varepsilon_{11}^a}{c_{33}}\end{cases} \tag{A3}$$

The vanishing membrane force, $\int_h \sigma_{11}^a dz = 0$, gives ε_{33}^a. Its integration then leads to the expansion of the actuator Δu in Eq. (1).

For the pressure q_i on the ith sensor and the vanishing stress and electric displacement fields $\sigma_{33}^i = q_i$ and $D_3^i = 0$ (where the superscript i denotes the ith sensor), Eqs. (A1) and (A2), together with the vanishing of membrane force, $\int_h \sigma_{11}^i dz = 0$, give the following equations to determine ε_{11}^i, ε_{33}^i, and E_3^i :

$$\begin{cases}0 = \dfrac{(c_{11}c_{33}-c_{13}^2)\varepsilon_{11}^i + (c_{13}e_{33}-c_{33}e_{31})E_3^i + c_{13}q_i}{c_{33}}\\ \varepsilon_{33}^i = \dfrac{q_i + e_{33}E_3^i - c_{13}\varepsilon_{11}^i}{c_{33}}\\ e_{31}\varepsilon_{11}^i + e_{33}\varepsilon_{33}^i + k_{33}E_3^i = 0\end{cases} \tag{A4}$$

This gives the output voltage $U_{S,i} = |E_3^i| \cdot h$ in Eq. (9). The expansion $\Delta u_i = \varepsilon_{33}^i \cdot h$ of the ith sensor is

$$\Delta u_i = \frac{\left(c_{11}k_{33} + e_{31}^2\right)q_i h}{c_{11}e_{33}^2 + c_{11}c_{33}k_{33} + c_{33}e_{31}^2 - 2c_{13}e_{31}e_{33} - c_{13}^2 k_{33}} \tag{A5}$$

Its ratio to the expansion of the actuator given in Eq. (1) is then given by

$$\frac{\Delta u_i}{\Delta u} = \frac{E'h}{8b\pi} \frac{c_{11}k_{33} + e_{31}^2}{c_{11}e_{33}^2 + c_{11}c_{33}k_{33} + c_{33}e_{31}^2 - 2c_{13}e_{31}e_{33} - c_{13}^2 k_{33}} \ln\left[\frac{1}{1 - \dfrac{b^2}{i^2(b+w)^2}}\right] \tag{A6}$$

which is extremely small as illustrated in main text.

References

[1] Escoffier, C., Derigal, J., Rochefort, A., Vasselet, R., Leveque, J. L., and Agache, P. G., 1989, "Age-Related Mechanical Properties of Human Skin: An In Vivo Study," J. Invest. Dermatol., **93**(3), pp. 353–357.

[2] Pailler-Mattei, C., Bec, S., and Zahouani, H., 2008, "In Vivo Measurements of the Elastic Mechanical Properties of Human Skin by Indentation Tests," Med. Eng. Phys., **30**(5), pp. 599–606.

[3] Agache, P. G., Monneur, C., Leveque, J. L., and De Rigal, J., 1980, "Mechanical Properties and Young's Modulus of Human Skin In Vivo," Arch. Dermatol. Res., **269**(3), pp. 221–232.

[4] Diridollou, S., Patat, F., Gens, F., Vaillant, L., Black, D., Lagarde, J. M., Gall, Y., and Berson, M., 2000, "In Vivo Model of the Mechanical Properties of the Human Skin Under Suction," Skin Res. Technol., **6**(4), pp. 214–221.

[5] Dagdeviren, C., Shi, Y., Joe, P., Ghaffari, R., Balooch, G., Usgaonkar, K., Gur, O., Tran, P. L., Crosby, J. R., Meyer, M., Su, Y., Webb, R. C., Tedesco, A. S., Slepian, M. J., Huang, Y., and Rogers, J. A., 2015, "Conformal Piezoelectric Systems for Clinical and Experimental Characterization of Soft Tissue Biomechanics," Nat. Mater. (in press).

[6] Dagdeviren, C., Yang, B. D., Su, Y., Tran, P. L., Joe, P., Anderson, E., Xia, J., Doraiswamy, V., Dehdashti, B., Feng, X., Lu, B., Poston, R., Khalpey, Z., Ghaffari, R., Huang, Y., Slepian, M. J., and Rogers, J. A., 2014, "Conformal Piezoelectric Energy Harvesting and Storage From Motions of the Heart, Lung, and Diaphragm," Proc. Natl. Acad. Sci. USA, **111**(5), pp. 1927–1932.

[7] Huang, Y., Zhou, W. X., Hsia, K. J., Menard, E., Park, J. U., Rogers, J. A., and Alleyne, A. G., 2005, "Stamp Collapse in Soft Lithography," Langmuir, **21**(17), pp. 8058–8068.

[8] Tada, H., Paris, P. C., and Irwin, G. R., 2000, *The Stress Analysis of Cracks Handbook*, 3rd ed., ASME Press, New York.

[9] Muskhelishvili, N. I., 1953, *Some Basic Problems of the Mathematical Theory of Elasticity*, P. Noordhoff Ltd., Amsterdam.

[10] Wang, L., and Lin, X., 1985, "Problems on Infinite Plate With Arbitrary Collinear Cracks," Acta Mech. Sin., **17**(3), pp. 243–252.

[11] Fang, D., and Liu, J., 2014, *Fracture Mechanics of Piezoelectric and Ferroelectric Solids*, Tsinghua University Press/Springer, Beijing.